EUROPEAN ORGANIZATION FOR NUCLEAR RESEARCH

CERN-EP/98-148
21 September 1998

QCD Results from Studies of Hadronic Events produced in e^+e^- Annihilations at $\sqrt{s} = 183$ GeV

L3 Collaboration

Abstract

We present results obtained from a study of the structure of hadronic events recorded by the L3 detector at a centre-of-mass energy of 183 GeV. The data sample corresponds to an integrated luminosity of 55.3 pb^{-1}. The distributions of event shape variables and the energy dependence of their mean values are measured. From a comparison with resummed $\mathcal{O}(\alpha_s^2)$ QCD calculations, we determine the strong coupling constant α_s (183 GeV) $= 0.1086 \pm 0.0026\ (exp) \pm 0.0054\ (th)$. The charged particle multiplicity distribution and momentum spectrum are studied and the energy dependence of the peak position of the $\xi\ (= -\ln x_p)$ distribution is compared with lower energy measurements and QCD expectations.

Submitted to *Phys. Lett. B*

Introduction

Hadronic events produced in e^+e^- annihilation offer a good environment to test the predictions of the theory of the strong interaction (QCD) [1]. Each time a new collision energy is available it is important to study the main characteristics of the hadronic events not only for testing QCD predictions but also for checking the validity of the QCD models very often used in particle searches and other studies. In 1997 the centre-of-mass energy of LEP was increased to 183 GeV. We report here on the studies of several event shape variables for the high energy hadronic final states from the data, corresponding to an integrated luminosity of 55.3 pb^{-1}, collected with the L3 detector [2, 3]. To allow a direct comparison with our earlier QCD tests done at lower energies [4, 5], we follow an identical analysis procedure.

The first part of the work consists of comparing measured event shape variable distributions with QCD models with parameters tuned using hadronic Z decays [6].

The strong coupling constant is then determined at 183 GeV by comparing the measured distributions of event shape variables with the predictions of a second order QCD calculation with resummed leading and next-to-leading terms. The experimental uncertainty obtained at this new energy is smaller than for previous high energy measurements done above the Z, due to the higher luminosity collected.

We include the measurement of the charged particle multiplicity distributions and the peak position, $\xi^\star$, of the charged particle ξ $(= -\ln x_p)$ spectrum at 183 GeV together with similar measurements at 133, 161 and 172 GeV.

Selection of Hadronic Events

The selection of $e^+e^- \to$ hadrons events is based on the energy measured in the electromagnetic calorimeter composed of BGO crystals and in the uranium hadron calorimeter with proportional wire chamber readout [2,3]. We use energy clusters in the calorimeters with a minimum energy of 100 MeV. The number of clusters is denoted by $N_{\rm cl}$. We measure the total visible energy ($E_{\rm vis}$) and the energy imbalance parallel ($E_\parallel$) and perpendicular ($E_\perp$) to the beam direction. The hadronic event selection is identical to the selection at $\sqrt{s} = 172$ GeV [5].

Monte Carlo events of the process $e^+e^- \to q\bar{q}(\gamma)$ have been generated by the parton shower program PYTHIA 5.7 [7] and passed through the L3 detector simulation [8].

Above the Z pole a large fraction of the events are accompanied by a photon from hard initial state radiation (ISR). The fraction of such events in our sample is about 55%. To reduce this contamination, we apply the two cuts used at 172 GeV which are:

- $(E_{vis}/\sqrt{s}) > 2.0(\mid E_\parallel \mid /E_{vis}) + 0.5$
- energy of the most energetic photon, $E_\gamma, < 30$ GeV.

The first cut uses the correlation between $E_{vis}/\sqrt{s}$ and $\mid E_\parallel \mid /E_{vis}$ to discriminate well balanced events from unbalanced events arising from an ISR photon lost in the beam pipe. The events where the photon from initial state radiation is seen in the detector are removed by the second cut. A sample of 2010 events is selected. Applying these cuts to the simulated events we find that 88% of the events with no hard initial state radiation greater than 30 GeV are accepted. The dominant source of background at this energy comes from hadronic decays of W pairs. It amounts to about 25% at this level of selection. Before doing a background subtraction, a substantial fraction of this contamination (more than 50%) is removed using a specific W^+W^- event selection similar to the one described in reference [5]. The selection, based on the 4 jet topology, has been optimised for 183 GeV and the new cuts are:

$N_{\rm cl} \geq 40$; $N_{\rm tr} > 15$
$E_{\rm jet1} < 0.405\sqrt{s}$; $E_{\rm jet4} > 0.055\sqrt{s}$
$y_{34}^{\rm D} \geq 0.006$; $\mid E_{\parallel} \mid /E_{\rm vis} < 0.2$

where $y_{34}^{\rm D}$ is the jet resolution parameter in Durham algorithm [9] for which the event goes from a four-jet to a three-jet topology and $N_{\rm tr}$ is the number of tracks measured in the central tracking chamber. The tracks are required to have at least 30 hits and a transverse momentum greater than 100 MeV. $E_{\rm jet1}$ and $E_{\rm jet4}$ are the rescaled energies of the most and the least energetic jets when the events are forced to form four jets using the Durham algorithm.

After this additional rejection the final sample at 183 GeV contains 1619 events. This corresponds to an efficiency of 84.4% to select hadronic events with no hard ISR with energy greater than 30 GeV and a purity of 74.1%. Contaminations from ISR and $\rm W^+W^-$ events have been estimated to be 10.2% and 11.7% respectively. Table 1 summarises the background content of the remaining event sample. For the background studies the following Monte Carlo programs were used: KORALZ [10] ($\rm e^+e^- \to \tau^+\tau^-(\gamma)$), KORALW [11] ($\rm e^+e^- \to W^+W^- \to f\,f'f\,f'$), BHAGENE3 [12] ($\rm e^+e^- \to e^+e^-(\gamma)$), PYTHIA ($\rm e^+e^- \to ZZ$, $\rm e^+e^- \to Ze^+e^-$), PYTHIA and PHOJET [13] ($\rm e^+e^- \to$ hadrons $\rm e^+e^-$).

Measurement of event shape variables

We measure five variables, thrust (T), scaled heavy jet mass (ρ), total ($B_{\rm T}$) and wide ($B_{\rm W}$) jet broadening variables and the C-parameter, for which improved analytical QCD calculations are available [14–18].

Thrust: The global event shape variable thrust, T, [19] is defined as:

$$T \;=\; \max \frac{\sum |\vec{p}_i \cdot \vec{n}_T|}{\sum |\vec{p}_i|} \;,$$

where $\vec{p}_i$ is the momentum vector of the particle i. The thrust axis $\vec{n}_T$ is the unit vector which maximises the above expression. The value of the thrust can vary between 0.5 and 1.

Scaled heavy jet mass: The heavy jet mass M_H is defined as: [20]

$$M_H \;=\; \max[M_+(\vec{n}_T), M_-(\vec{n}_T)] \;,$$

where $M_\pm$ are the invariant masses in the two hemispheres, $S_\pm$, defined by the plane normal to the thrust axis:

$$M_\pm^2 \;=\; \left(\sum_{i \in S_\pm} p_i\right)^2$$

where p_i is the four momentum of particle i. The scaled heavy jet mass ρ is defined as:

$$\rho \;=\; M_H^2/s \;.$$

Jet broadening variables: These variables are defined [16] by computing in the hemispheres $S_\pm$ the quantities:

$$B_\pm \;=\; \frac{\sum_{i \in S_\pm} |\vec{p}_i \times \vec{n}_T|}{2 \sum_i |\vec{p}_i|} \;.$$

The observables used to study α_s are

$$B_T = B_+ + B_- \quad \text{and} \quad B_W = \max(B_+, B_-)$$

referred to as 'total jet broadening' and 'wide jet broadening', respectively.

***C*-Parameter:** The C parameter is derived from the eigenvalues of the spherocity tensor [21]:

$$\theta^{ij} = \frac{\sum_a p_a^i p_a^j / \mid \vec{p_a} \mid}{\sum_a \mid \vec{p_a} \mid} \quad i,j = 1,2,3 \ ;$$

It is defined in terms of the eigenvalues of θ^{ij}, λ_1, λ_2, and λ_3, as:

$$C = 3(\lambda_1\lambda_2 + \lambda_2\lambda_3 + \lambda_3\lambda_1) \ ;$$

For Monte Carlo events, the global event shape variables are calculated before (particle level) and after (detector level) detector simulation. The calculation before detector simulation takes into account all stable charged and neutral particles. The measured distributions at detector level differ from the ones at particle level because of detector effects, limited acceptance and resolution.

After subtracting the background events according to standard cross sections the measured distributions are corrected for detector effects, acceptance and resolution on a bin-by-bin basis by comparing the detector level results with the particle level results. We also correct the data for initial and final state photon radiation bin-by-bin using PYTHIA [7] Monte Carlo distributions at particle level with and without radiation.

Figure 1 shows the corrected thrust and wide jet broadening distributions obtained at $\sqrt{s} =$ 183 GeV. The data are compared with JETSET 7.4 [22], HERWIG 5.6 [23], ARIADNE 4.06 [24] and COJETS 6.23 [25] QCD models at particle level without ISR. The agreement is good. The figure also shows the various corrections applied at detector level to obtain the final distribution. Typical correction factors for resolution as well as for acceptance and initial state radiation are between 0.5 and 1.5.

The systematic errors in the distributions of event shape variables arise mainly due to uncertainties in detector calibration and those in estimating the background.

The effect of detector calibration is studied by changing the definition of reconstructed objects used in the detector to calculate the observables. Instead of using only calorimetric clusters, the analysis has been repeated with objects obtained from a non-linear combination of energies of charged tracks and calorimetric clusters. The effect due to possible inhomogeneities in the detector response is estimated by comparing the results with those obtained by restricting the events to the central part of the detector where the resolution is better ($|\cos(\theta_T)| < 0.7$, where θ_T is the polar angle of the thrust axis relative to the beam direction).

The uncertainty on the background composition of the selected event sample has been estimated by repeating the analysis with:

- an alternative criterion to reject the hard initial state photon events based on a cut on the effective centre-of-mass energy reconstructed from kinematical considerations. The cut corresponds to $\sqrt{s'/s} > 0.92$
- an alternative W^+W^- background treatment based on subtraction without the W^+W^- rejection cuts.

- variation of the estimated 2-photon interaction background by $\pm$ 30%.

We also vary the MC model (HERWIG [23] instead of JETSET [22]) used to correct the distributions. The final systematic error is taken as the sum in quadrature of all the contributions mentioned above.

Energy Dependence of Mean Values

An important test of QCD models is a comparison of the energy evolution of the event shape variables. The measured mean values of thrust, scaled heavy jet mass, total jet broadening, wide jet broadening and C-parameter are summarised in Table 2. The energy dependence of the mean event shape variables arises mainly from two sources: the logarithmic energy scale dependence of α_s and the power law behaviour of the non-perturbative effects. As an example, the mean values of $(1-T)$ and wide jet broadening B_W are shown in Figure 2, together with those measured at the Z resonance [26, 27], above the Z [4, 5, 28], and at low energy e^+e^- machines [29]. Also shown are the energy dependences of these quantities as predicted by JETSET 7.4 PS [22], HERWIG 5.6, ARIADNE 4.06, COJETS 6.23 and JETSET 7.4 ME Monte Carlo models with constant parameter values over the entire energy range. These models have been tuned [6] to global event shape distributions and charged particle multiplicity distributions measured at 91.2 GeV. They use different approaches to describe the perturbative and non-perturbative phase of QCD evolution. For both the distributions all the models, with the exception of JETSET ME, agree well with the data.

α_s Determination

In order to derive α_s, we fit the measured distributions of the event shape variables to theoretical calculations based on $\mathcal{O}(\alpha_s^2)$ perturbative QCD with resummed leading and next-to-leading order terms. These calculations are performed at parton level and do not include heavy quark mass effects. To compare the analytical calculations with the experimental distributions, the effect of hadronisation and decays has been corrected using Monte Carlo programs.

For the fit, we need to define ranges that take into account the limited statistics at LEP2 as well as the reliability of the resummation calculation. The fit ranges given in Table 3 are the same as those in our earlier analyses [4, 5]. We carry out fits to the C-parameter for the first time to extract the value of α_s.

Figure 3 shows the experimental data together with the QCD fits for the five variables T, ρ, B_T, B_W and C. The corresponding α_s values obtained from the fits to the distributions are presented in Table 3 with the experimental and theoretical errors.

The experimental error corresponds to the statistical errors together with the experimental systematic uncertainties estimated by varying the energy calibration and background content as mentioned earlier.

The theoretical error is obtained from an estimate of the hadronization uncertainty and of the errors coming from the uncalculated higher orders in the QCD predictions. The first part of Table 4 shows the variation in the fitted value of α_s due to different hadronisation corrections. The hadronisation correction using JETSET has been taken as a reference point. α_s has been determined using different hadronisation models (HERWIG, ARIADNE) and changing several parameters of JETSET. For all variables but the wide jet broadening (B_W), the most important

variation comes from the change in the fragmentation models. We use this as an estimate of the overall hadronisation uncertainty.

The second part of the table summarises the errors coming from uncalculated higher orders in the QCD predictions. The scale error is obtained by repeating the fit for different values of the renormalisation scale in the interval $0.5\sqrt{s} \leq \mu \leq 2\sqrt{s}$. For all these scales a good fit is obtained. The matching scheme uncertainty is obtained from half of the maximum spread due to the variation of the matching algorithm [30]. The systematic errors due to uncalculated higher order terms have been estimated independently from the scale uncertainty and the matching scheme uncertainty. The largest of these is taken as the theoretical uncertainty due to uncalculated higher orders. The overall theoretical error for each event shape variable is obtained by adding to this in quadrature the hadronisation uncertainty.

One should note that this estimate of the theoretical error may not always reflect on the true size of uncalculated higher order terms. It is better to compare α_s measurements from many event shape variables which are affected differently by higher order corrections and hadronisation effects. To obtain a combined value for the strong coupling constant we take the unweighted average of the five α_s values. We estimate the overall theoretical error from the simple average of the five theoretical errors or from half of the maximum spread in the five α_s values. Both these estimates yield similar results. The combined results are:

$$\alpha_s\ (183\ \ \mathrm{GeV}) \ = \ 0.1083 \ \pm \ 0.0028\ (\mathrm{exp}) \ \pm \ 0.0054\ (\mathrm{th})$$

where the first error is experimental and the second error is theoretical.

We have examined the dependence of the value of α_s on the fit range. We repeated the α_s determination with a new set of ranges also given in Table 3 where we excluded the extreme 2-jet region. We find α_s (183 GeV) = 0.1083 $\pm$ 0.0093 (exp) $\pm$ 0.0046 (th) in agreement with the earlier number. The number of events contributing to the new fits is drastically reduced resulting in a large statistical error. The estimated experimental systematic error also increases.

To compare the α_s value with our earlier measurements done at lower energies [4, 5, 31, 32], we use the mean α_s value measured from four event shape variables, T, ρ, B_T and B_W:

$$\alpha_s\ (183\ \ \mathrm{GeV}) \ = \ 0.1086 \ \pm \ 0.0026\ (\mathrm{exp}) \ \pm \ 0.0054\ (\mathrm{th})$$

The most precise measurements of α_s come from the determination at $\sqrt{s} = M_Z$ and at 183 GeV. It should be noted that the theoretical errors are strongly correlated between these measurements. The higher order uncertainties should be the same and the uncertainties due to hadronisation corrections are comparable at these energies. The error appropriate to a measurement of the energy dependence of α_s can then be considered to be purely experimental.

The experimental systematic errors on α_s are dominated by the background uncertainties. These are similar for all the individual low energy or high energy data points but differ between the low energy, Z peak and high energy data sets. The experimental systematic errors are then different and uncorrelated between the three data sets, but are taken as fully correlated between individual low energy or high energy measurements. The eleven measurements in Figure 4 are shown with experimental errors only, together with a fit to the QCD evolution equation with $\alpha_s(M_Z)$ as a free parameter. The fit gives a χ^2 of 16.9 for 10 degrees of freedom corresponding to a confidence level of 7.6% with a fitted value of α_s:

$$\alpha_s(M_Z) \ = \ 0.1216 \ \pm \ 0.0017\ (\mathrm{exp}) \ \pm \ 0.0058\ (\mathrm{th}).$$

On the other hand, a model with constant α_s gives a χ^2 of 91.4.

Charged Particle Multiplicity

The dynamics of hadron production can be probed using the charged particle multiplicity distribution which has been found to be sensitive to the parameters of the QCD models. Figure 5 shows the measured multiplicity distribution at detector level compared with Monte Carlo predictions for signal and background processes at $\sqrt{s} = 183$ GeV.

The measured distributions are corrected for the remaining estimated background using Monte Carlo on a bin-by-bin basis. The distributions are then corrected for resolution and acceptance, using a matrix unfolding method. In this correction procedure, we assume all weakly decaying light particles with mean lifetime larger than 3.3×10^{-10} s to be stable.

The systematic errors have been determined in the same manner as for the global event shape variables with one additional contribution corresponding to a variation of the quality criteria for track selection.

The first three moments of charged particle multiplicity distribution are summarised in Table 5 together with the dispersion and skewness variable.

Figure 6 shows the evolution of mean charged particle multiplicity with centre-of-mass energy compared to several QCD models. We also include measurements done by other e^+e^- experiments at similar [4, 5, 27, 28, 33] and lower [29] centre-of-mass energies. The parameters of these models are the same at all energies. We find that the energy dependence of the multiplicity distribution is in agreement with the predictions of parton shower models like JETSET [22], HERWIG [23], ARIADNE [24] which include QCD coherence effects. However, parton shower models with no QCD coherence effects like COJETS [25] or matrix element models as implemented in JETSET cannot explain the energy dependence. COJETS predicts a faster energy evolution, while the matrix element model, which has low parton multiplicity before fragmentation due to the $\mathcal{O}(\alpha_s^2)$ calculation, needs retuning at each centre-of-mass energy.

Inclusive Particle Spectrum

The phenomenon of colour coherence in QCD implies destructive interference in soft gluon emission. This gives rise to a suppression of hadron production at small momenta. We study the charged particle momentum spectrum in terms of the variable $\xi = \ln(1/x_p)$, where x_p is the momentum scaled by the beam energy. The observed distribution is corrected for the effect of background, detector resolution and acceptance on a bin-by-bin basis using Monte Carlo events. The corrected spectrum is shown in Figure 7. The asymptotic behaviour of the ξ spectrum is predicted to be Gaussian [34, 35]. Next-to-leading order corrections [36] distort the gaussian shape of the ξ distribution. This implies a narrower ξ-peak shifted towards lower x-values, skewed and flattened towards higher x-values, with the tail falling off faster than Gaussian. The smooth lines in Figure 7 are fits to the corrected distributions to a Gaussian and a skewed Gaussian function restricting the fit range to values of ξ where the distribution falls to 60% of its maximum value. During the fit, the statistical errors on the measurements are taken to be uncorrelated whereas the systematic errors are taken to be maximally correlated. Both the distributions give reasonable description of the data around the peak position suggesting that the next-to-leading corrections do not influence the determination of peak position at high energies. The fit to the skewed Gaussian distribution yields a χ^2 of 8.8 for 13 degrees of freedom and the peak position $\xi^\star$ in the ξ distribution is determined to be:

$$\xi^\star(183 \ \text{GeV}) \ = \ 4.075 \pm 0.022 \pm 0.038$$

where the first error is statistical and the second error is due to systematics. To estimate the systematic errors, we have repeated the fits changing (a) the functional form (Gaussian instead of skewed Gaussian); (b) the quality cuts on track selection; (c) the hadronic selection criteria to vary the backgrounds within one σ; (d) the model (HERWIG [23]) used for detector corrections (the default being PYTHIA). Half of the maximum spread is assigned as the systematic error. The $\xi^\star$ analysis has been repeated on the L3 data at lower centre-of-mass energies. The values obtained are summarised in Table 6.

Figure 8 shows the measured values of $\xi^\star$ together with earlier measurements [37–41] as a function of centre-of-mass energy. The energy evolution of $\xi^\star$ has been fitted using the QCD prediction [42]:

$$\xi^\star(s) \;=\; Y\left(\frac{1}{2} + a\sqrt{\frac{\alpha_{\rm s}(Y)}{32{\rm N_c}\pi}} - a^2\frac{\alpha_{\rm s}(Y)}{32{\rm N_c}\pi}\right),$$

where $Y = \ln(\sqrt{s}/2\Lambda)$, $a = (11/3{\rm N_c})+(2{\rm N_f}/3{\rm N_c}^2)$, $\alpha_{\rm s}(Y) = 2\pi/bY$ with $b = (11{\rm N_c}/3)-(2{\rm N_f}/3)$, $\rm N_c$ and $\rm N_f$ are number of colours and active flavours respectively. The first term is given by the double logarithm approximation (DLA), and the correction terms arise in the next-to-leading order (MLLA) QCD predictions. In the fits, we have taken the statistical error as fully uncorrelated and the systematic errors from the same experiment as fully correlated. The correlation of systematic errors among different experiments has been ignored.

We find that the data are in better agreement with QCD predictions computed to the next-to leading orders. The fit of the L3 and TASSO data to the DLA parametrisation gives a χ^2 of 34.7 for 8 degree of freedom (CL = 3.0×10^{-5}) whereas the MLLA predictions give a fit with χ^2 of 7.7 for 8 degrees of freedom (CL = 0.46).

It should be recalled that the suppression of hadron production at very small momenta resulting in a bell shape of the ξ distribution is expected on purely kinematical grounds due to finite hadron masses. Soft gluon coherence, however, increases this suppression and is manifested in the energy dependence of $\xi^\star$. The change with energy would be approximately two times larger without any destructive interference.

Summary

We have measured distributions of event shape variables in hadronic events from $\rm e^+e^-$ annihilation at $\sqrt{s} = 183$ GeV. The distributions of the event shape variables as well as the energy dependence of the mean are well described by QCD parton shower models.

The event shape distributions are compared to second order QCD calculations together with resummed leading and next-to-leading log terms. The data are well described by these calculations with a value of $\alpha_{\rm s} = 0.1086 \pm 0.0026$ (exp) $\pm$ 0.0054 (th) at $\sqrt{s} = 183$ GeV. This measurement together with our earlier measurements at lower centre-of-mass energies clearly demonstrates the running of $\alpha_{\rm s}$ as expected in QCD.

The energy evolution of the charged particle multiplicity as well as the inclusive charged particle momentum spectrum give evidence of soft gluon suppression. The energy evolution of the peak position $\xi^\star$ of inclusive ξ spectrum is described adequately by the next-to-leading order QCD calculation including interference effects.

References

[1] M. Gell-Mann, Acta Phys. Austriaca Suppl. **IX** (1972) 733;
H. Fritzsch and M. Gell-Mann, 16th International Conference on High Energy Physics, Batavia, 1972; editors J. D. Jackson and A. Roberts, National Accelerator Laboratory (1972);
H. Fritzsch, M. Gell-Mann and H. Leytwyler, Phys. Lett. **B47** (1973) 365;
D.J. Gross and F. Wilczek, Phys. Rev. Lett. **30** (1973) 1343;
D.J. Gross and F. Wilczek, Phys. Rev. **D8** (1973) 3633;
H.D. Politzer, Phys. Rev. Lett. **30** (1973) 1346;
G. 't Hooft, Nucl. Phys. **B33** (1971) 173.

[2] L3 Collaboration, B. Adeva *et al.*, Nucl. Inst. Meth. **A289** (1990) 35;
M. Chemarin *et al.*, Nucl. Inst. Meth. **A349** (1994) 345;
M. Acciarri *et al.*, Nucl. Inst. Meth. **A351** (1994) 300;
G. Basti *et al.*, Nucl. Inst. Meth. **A374** (1996) 293;
A. Adam *et al.*, Nucl. Inst. Meth. **A383** (1996) 342.

[3] L3 Collaboration, O. Adriani *et al.*, Phys. Rep., **236** (1993) 1.

[4] L3 Collaboration, M. Acciarri *et al.*, Phys. Lett. **B371** (1996) 137.

[5] L3 Collaboration, M. Acciarri *et al.*, Phys. Lett. **B404** (1997) 390.

[6] Sunanda Banerjee, Swagato Banerjee, L3 note 1978 (1996).

[7] PYTHIA 5.7 Monte Carlo Program:
QCD parton shower and fragmentation process are taken from JETSET 7.4 [22];
T. Sjöstrand, CERN-TH-7112/93 (1993), revised august 1995;
T. Sjöstrand, Comp. Phys. Comm. **82** (1994) 74.

[8] The L3 detector simulation is based on GEANT Version 3.15.
See R. Brun *et al.*, "GEANT 3", CERN DD/EE/84-1 (Revised), September 1987.
The GHEISHA program (H. Fesefeldt, RWTH Aachen Report PITHA 85/02 (1985)) is used to simulate hadronic interactions.

[9] Yu. L. Dokshitzer, Contribution to the Workshop on Jets at LEP and HERA (1990);
N. Brown and W.J. Stirling, Rutherford Preprint RAL-91-049;
S. Catani *et al.*, Phys. Lett. **B269** (1991) 432;
S. Bethke *et al.*, Nucl. Phys. **B370** (1992) 310.

[10] S. Jadach, B. F. L. Ward and Z. Wąs, Comp. Phys. Comm. **79** (1994) 503.

[11] M. Skrzypek *et al.*, Comp. Phys. Comm. **94** (1996) 216; Phys. Lett. **B372** (1996) 289.

[12] J. H. Field, Phys. Lett. **B323** (1994) 432; J. H. Field and T. Riemann, Comp.Phys.Comm. **94** (1996) 53.

[13] R. Engel, Z. Phys. **C66** (1995) 203; R. Engel, J. Ranft and S. Roesler, Phys. Rev. **D52** (1995) 1459.

[14] S. Catani *et al.*, Phys. Lett. **B263** (1991) 491.

[15] S. Catani *et al.*, Phys. Lett. **B272** (1991) 368.

[16] S. Catani *et al.*, Phys. Lett. **B295** (1992) 269.

[17] S. Bethke *et al.*, Nucl. Phys. **B370** (1992) 310.

[18] S. Catani and B.R. Webber, Phys. Lett. **B427** (1998) 377.

[19] S. Brandt *et al.*, Phys. Lett. **12** (1964) 57;
E. Fahri, Phys. Rev. Lett. **39** (1977) 1587.

[20] T. Chandramohan and L. Clavelli, Nucl. Phys. **B184** (1981) 365;
MARK II Collaboration, A. Peterson *et al.*, Phys. Rev. **D37** (1988) 1;
TASSO Collaboration, W. Braunschweig *et al.*, Z. Phys. **C45** (1989) 11.

[21] G. Parisi, Phys. Lett. **B74** (1978) 65;
J. F. Donoghue, F. E. Low, and S. Y. Pi, Phys. Rev. **D20** (1979) 2759.

[22] Jetset 7.4 Monte Carlo Program:
T. Sjöstrand, Comp. Phys. Comm. **39** (1986) 347;
T. Sjöstrand and M. Bengtsson, Comp. Phys. Comm. **43** (1987) 367.

[23] Herwig 5.6 Monte Carlo Program:
G. Marchesini and B. Webber, Nucl. Phys. **B310** (1988) 461;
I. G. Knowles, Nucl. Phys. **B310** (1988) 571;
G. Marchesini *et al.*, Comp. Phys. Comm. **67** (1992) 465.

[24] Ariadne 4.06 Monte Carlo Program:
U. Pettersson, "ARIADNE: A Monte Carlo for QCD Cascades in the Color Dipole Formulation", Lund Preprint, LU TP 88-5 (1988);
L. Lönnblad, "The Colour Dipole Cascade Model and the Ariadne Program", Lund Preprint, LU TP 91-11 (1991).

[25] Cojets 6.23 Monte Carlo Program:
R. Odorico, Nucl. Phys. **B228** (1983) 381;
R. Odorico, Comp. Phys. Comm. **32** (1984) 139, Erratum: **34** (1985) 43;
R. Mazzanti and R. Odorico, Nucl. Phys. **B370** (1992) 23; Bologna preprint DFUB 92/1.

[26] L3 Collaboration, B. Adeva *et al.*, Z. Phys. **C55** (1992) 39.

[27] ALEPH Collaboration, D. Decamp *et al.*, Phys. Lett. **B273** (1991) 181;
ALEPH Collaboration, D. Buskulic *et al.*, Z. Physik **C55** (1992) 209;
DELPHI Collaboration, P. Aarnio *et al.*, Phys. Lett. **B240** (1990) 271;
DELPHI Collaboration, P. Abreu *et al.*, Z. Phys. **C50** (1991) 185;
OPAL Collaboration, M. Z. Akrawy *et al.*, Z. Phys. **C47** (1990) 505;
OPAL Collaboration, P. D. Acton *et al.*, Z. Phys. **C53** (1992) 539.

[28] ALEPH Collaboration, D. Buskulic *et al.*, Z. Physik **C73** (1997) 409;
ALEPH Collaboration, R. Barate *et al.*, Phys. Rep. **294** (1998) 1;
DELPHI Collaboration, P. Abreu *et al.*, Phys. Lett. **B372** (1996) 172;
DELPHI Collaboration, P. Abreu *et al.*, Z. Physik **C73** (1997) 229;
DELPHI Collaboration, P. Abreu *et al.*, Phys. Lett. **B416** (1998) 233;

OPAL Collaboration, G. Alexander *et al.*, Z. Physik **C72** (1996) 191;
OPAL Collaboration, K. Ackerstaff *et al.*, Z. Physik **C75** (1997) 193.

[29] AMY Collaboration, Y. K. Li *et al.*, Phys. Rev. **D41** (1990) 2675;
AMY Collaboration, H. W. Zheng *et al.*, Phys. Rev. **D42** (1990) 737;
JADE Collaboration, W. Bartel *et al.*, Z. Phys. **C20** (1983) 187;
MARK J Collaboration, D. P. Barber *et al.*, Phys. Rev. Lett. **43** (1979) 901;
TASSO Collaboration, W. Braunschweig *et al.*, Z. Phys. **C45** (1989) 193;
TASSO Collaboration, W. Braunschweig *et al.*, Z. Phys. **C47** (1990) 187;
M. Yamauchi (TOPAZ Collaboration), 'Recent Results from TOPAZ at TRISTAN', 24th Int. Conf. on High Energy Physics, Munich 1988.

[30] S. Catani *et al.*, Nucl. Phys. **B407** (1993) 3.

[31] L3 Collaboration, O. Adriani *et al.*, Phys. Lett. **B284** (1992) 471.

[32] L3 Collaboration, M. Acciarri *et al.*, Phys. Lett. **B411** (1997) 339.

[33] L3 Collaboration, B. Adeva *et al.*, Phys. Lett. **B248** (1990) 464;
L3 Collaboration, B. Adeva *et al.*, Phys. Lett. **B284** (1992) 471;
L3 Collaboration, B. Adeva *et al.*, Z. Physik **C55** (1992) 39.

[34] A.H. Mueller, in *Proc. 1981 International Symposium on Lepton and Photon Interactions at High Energies*, ed. W. Pfeil (Bonn, 1981), p.689; Yu.L. Dokshitzer, V.S. Fadin and V.A. Khoze, Phys. Lett. **B115** (1982) 242.

[35] A. H. Mueller, Nucl. Phys. **B213** (1983) 85, *ibid.* **B241** (1984) 141.

[36] C. P. Fong and B. R. Webber, Phys. Lett. **B229** (1989) 289.

[37] L3 Collaboration, B. Adeva *et al.*, Phys. Lett. **B259** (1991) 199.

[38] TASSO Collaboration, W. Braunschweig *et al.*, Z. Physik **C47** (1990) 187.

[39] ALEPH Collaboration, R. Barate *et al.*, Phys. Rep. **294** (1998) 1.

[40] DELPHI Collaboration, P. Abreu *et al.*, Phys. Lett. **B275** (1992) 231;
DELPHI Collaboration, P. Abreu *et al.*, Z. Physik **C73** (1997) 229.

[41] OPAL Collaboration, M. Akrawy *et al.*, Phys. Lett. **B247** (1990) 617;
OPAL Collaboration, G. Alexander *et al.*, Z. Physik **C72** (1996) 191;
OPAL Collaboration, K. Ackerstaff *et al.*, Z. Physik **C75** (1997) 193.

[42] Yu. L. Dokshitzer *et al.*, Basics of Perturbative QCD, Editions Frontieres, Gif-sur-Yvette, 1991.

The L3 Collaboration:

M.Acciarri,[28] O.Adriani,[17] M.Aguilar-Benitez,[27] S.Ahlen,[12] J.Alcaraz,[27] G.Alemanni,[23] J.Allaby,[18] A.Aloisio,[30] M.G.Alviggi,[30] G.Ambrosi,[20] H.Anderhub,[49] V.P.Andreev,[7,38] T.Angelescu,[14] F.Anselmo,[10] A.Arefiev,[29] T.Azemoon,[3] T.Aziz,[11] P.Bagnaia,[37] L.Baksay,[44] S.Banerjee,[11] Sw.Banerjee,[11] K.Banicz,[46] A.Barczyk,[49,47] R.Barillère,[18] L.Barone,[37] P.Bartalini,[23] A.Baschirotto,[28] M.Basile,[10] R.Battiston,[34] A.Bay,[23] F.Becattini,[17] U.Becker,[16] F.Behner,[49] J.Berdugo,[27] P.Berges,[16] B.Bertucci,[34] B.L.Betev,[49] S.Bhattacharya,[11] M.Biasini,[34] A.Biland,[49] G.M.Bilei,[34] J.J.Blaising,[4] S.C.Blyth,[35] G.J.Bobbink,[2] R.Bock,[1] A.Böhm,[1] L.Boldizsar,[15] B.Borgia,[18,37] D.Bourilkov,[49] M.Bourquin,[20] S.Braccini,[20] J.G.Branson,[40] V.Brigljevic,[49] I.C.Brock,[35] A.Buffini,[17] A.Buijs,[45] J.D.Burger,[16] W.J.Burger,[34] J.Busenitz,[44] A.Button,[3] X.D.Cai,[16] M.Campanelli,[49] M.Capell,[16] G.Cara Romeo,[10] G.Carlino,[30] A.M.Cartacci,[17] J.Casaus,[27] G.Castellini,[17] F.Cavallari,[37] N.Cavallo,[30] C.Cecchi,[20] M.Cerrada,[27] F.Cesaroni,[24] M.Chamizo,[27] Y.H.Chang,[51] U.K.Chaturvedi,[19] M.Chemarin,[26] A.Chen,[51] G.Chen,[8] G.M.Chen,[8] H.F.Chen,[21] H.S.Chen,[8] X.Chereau,[4] G.Chiefari,[30] C.Y.Chien,[5] L.Cifarelli,[39] F.Cindolo,[10] C.Civinini,[17] I.Clare,[16] R.Clare,[16] G.Coignet,[4] A.P.Colijn,[2] N.Colino,[27] S.Costantini,[9] F.Cotorobai,[14] B.de la Cruz,[27] A.Csilling,[15] T.S.Dai,[16] R.D'Alessandro,[17] R.de Asmundis,[30] A.Degré,[4] K.Deiters,[47] D.della Volpe,[30] P.Denes,[36] F.DeNotaristefani,[37] M.Diemoz,[37] D.van Dierendonck,[2] F.Di Lodovico,[49] C.Dionisi,[18,37] M.Dittmar,[49] A.Dominguez,[40] A.Doria,[30] M.T.Dova,[19,♯] D.Duchesneau,[4] P.Duinker,[2] I.Duran,[41] S.Easo,[34] H.El Mamouni,[26] A.Engler,[35] F.J.Eppling,[16] F.C.Erné,[2] P.Extermann,[20] M.Fabre,[47] R.Faccini,[37] M.A.Falagan,[27] S.Falciano,[37] A.Favara,[17] J.Fay,[26] O.Fedin,[38] M.Felcini,[49] T.Ferguson,[35] F.Ferroni,[37] H.Fesefeldt,[1] E.Fiandrini,[34] J.H.Field,[20] F.Filthaut,[18] P.H.Fisher,[16] I.Fisk,[40] G.Forconi,[16] L.Fredj,[20] K.Freudenreich,[49] C.Furetta,[28] Yu.Galaktionov,[29,16] S.N.Ganguli,[11] P.Garcia-Abia,[6] M.Gataullin,[33] S.S.Gau,[13] S.Gentile,[37] N.Gheordanescu,[14] S.Giagu,[37] S.Goldfarb,[23] J.Goldstein,[12] Z.F.Gong,[21] A.Gougas,[5] G.Gratta,[33] M.W.Gruenewald,[9] R.van Gulik,[2] V.K.Gupta,[36] A.Gurtu,[11] L.J.Gutay,[46] D.Haas,[6] B.Hartmann,[1] A.Hasan,[31] D.Hatzifotiadou,[10] T.Hebbeker,[9] A.Hervé,[18] P.Hidas,[15] J.Hirschfelder,[35] W.C.van Hoek,[32] H.Hofer,[49] H.Hoorani,[35] S.R.Hou,[51] G.Hu,[5] I.Iashvili,[48] B.N.Jin,[8] L.W.Jones,[3] P.de Jong,[18] I.Josa-Mutuberria,[27] R.A.Khan,[19] D.Kamrad,[48] J.S.Kapustinsky,[25] M.Kaur,[19,◇] M.N.Kienzle-Focacci,[20] D.Kim,[37] D.H.Kim,[43] J.K.Kim,[43] S.C.Kim,[43] W.W.Kinnison,[25] A.Kirkby,[33] D.Kirkby,[33] J.Kirkby,[18] D.Kiss,[15] W.Kittel,[32] A.Klimentov,[16,29] A.C.König,[32] A.Kopp,[48] I.Korolko,[29] V.Koutsenko,[16,29] R.W.Kraemer,[35] W.Krenz,[1] A.Kunin,[16,29] P.Lacentre,[48,♮,♯] P.Ladron de Guevara,[27] I.Laktineh,[26] G.Landi,[17] C.Lapoint,[16] K.Lassila-Perini,[49] P.Laurikainen,[22] A.Lavorato,[39] M.Lebeau,[18] A.Lebedev,[16] P.Lebrun,[26] P.Lecomte,[49] P.Lecoq,[18] P.Le Coultre,[49] H.J.Lee,[9] J.M.Le Goff,[18] R.Leiste,[48] E.Leonardi,[37] P.Levtchenko,[38] C.Li,[21] C.H.Lin,[51] W.T.Lin,[51] F.L.Linde,[2,18] L.Lista,[30] Z.A.Liu,[8] W.Lohmann,[48] E.Longo,[37] W.Lu,[33] Y.S.Lu,[8] K.Lübelsmeyer,[1] C.Luci,[18,37] D.Luckey,[16] L.Luminari,[37] W.Lustermann,[49] W.G.Ma,[21] M.Maity,[11] G.Majumder,[11] L.Malgeri,[18] A.Malinin,[29] C.Maña,[27] D.Mangeol,[32] P.Marchesini,[49] G.Marian,[44,¶] A.Marin,[12] J.P.Martin,[26] F.Marzano,[37] G.G.G.Massaro,[2] K.Mazumdar,[11] R.R.McNeil,[7] S.Mele,[18] L.Merola,[30] M.Meschini,[17] W.J.Metzger,[32] M.von der Mey,[1] D.Migani,[10] A.Mihul,[14] A.J.W.van Mil,[32] H.Milcent,[18] G.Mirabelli,[37] J.Mnich,[18] P.Molnar,[9] B.Monteleoni,[17] R.Moore,[3] T.Moulik,[11] R.Mount,[33] G.S.Muanza,[26] F.Muheim,[20] A.J.M.Muijs,[2] S.Nahn,[16] M.Napolitano,[30] F.Nessi-Tedaldi,[49] H.Newman,[33] T.Niessen,[1] A.Nippe,[23] A.Nisati,[37] H.Nowak,[48] Y.D.Oh,[43] G.Organtini,[37] R.Ostonen,[22] C.Palomares,[27] D.Pandoulas,[1] S.Paoletti,[37,18] P.Paolucci,[30] H.K.Park,[35] I.H.Park,[43] G.Pascale,[37] G.Passaleva,[18] S.Patricelli,[30] T.Paul,[13] M.Pauluzzi,[34] C.Paus,[18] F.Pauss,[49] D.Peach,[18] M.Pedace,[37] Y.J.Pei,[1] S.Pensotti,[28] D.Perret-Gallix,[4] B.Petersen,[32] S.Petrak,[9] A.Pevsner,[5] D.Piccolo,[30] M.Pieri,[17] P.A.Piroué,[36] E.Pistolesi,[28] V.Plyaskin,[29] M.Pohl,[49] V.Pojidaev,[29,17] H.Postema,[16] J.Pothier,[18] N.Produit,[20] D.Prokofiev,[38] J.Quartieri,[39] G.Rahal-Callot,[49] N.Raja,[11] P.G.Rancoita,[28] M.Rattaggi,[28] G.Raven,[40] P.Razis,[31] D.Ren,[49] M.Rescigno,[37] S.Reucroft,[13] T.van Rhee,[45] S.Riemann,[48] K.Riles,[3] A.Robohm,[49] J.Rodin,[44] B.P.Roe,[3] L.Romero,[27] S.Rosier-Lees,[4] S.Roth,[1] J.A.Rubio,[18] D.Ruschmeier,[9] H.Rykaczewski,[49] S.Sakar,[37] J.Salicio,[18] E.Sanchez,[27] M.P.Sanders,[32] M.E.Sarakinos,[22] C.Schäfer,[1] V.Schegelsky,[38] S.Schmidt-Kaerst,[1] D.Schmitz,[1] N.Scholz,[49] H.Schopper,[50] D.J.Schotanus,[32] J.Schwenke,[1] G.Schwering,[1] C.Sciacca,[30] D.Sciarrino,[20] L.Servoli,[34] S.Shevchenko,[33] N.Shivarov,[42] V.Shoutko,[29] J.Shukla,[25] E.Shumilov,[29] A.Shvorob,[33] T.Siedenburg,[1] D.Son,[43] B.Smith,[16] P.Spillantini,[17] M.Steuer,[16] D.P.Stickland,[36] A.Stone,[7] H.Stone,[36] B.Stoyanov,[42] A.Straessner,[1] K.Sudhakar,[11] G.Sultanov,[19] L.Z.Sun,[21] G.F.Susinno,[20] H.Suter,[49] J.D.Swain,[19] Z.Szillasi,[44,¶] X.W.Tang,[8] L.Tauscher,[6] L.Taylor,[13] C.Timmermans,[32] Samuel C.C.Ting,[16] S.M.Ting,[16] S.C.Tonwar,[11] J.Tóth,[15] C.Tully,[36] K.L.Tung,[8] Y.Uchida,[16] J.Ulbricht,[49] E.Valente,[37] G.Vesztergombi,[15] I.Vetlitsky,[29] G.Viertel,[49] S.Villa,[13] M.Vivargent,[4] S.Vlachos,[6] H.Vogel,[35] H.Vogt,[48] I.Vorobiev,[18,29] A.A.Vorobyov,[38] A.Vorvolakos,[31] M.Wadhwa,[6] W.Wallraff,[1] J.C.Wang,[16] X.L.Wang,[21] Z.M.Wang,[21] A.Weber,[1] S.X.Wu,[16] S.Wynhoff,[1] J.Xu,[12] Z.Z.Xu,[21] B.Z.Yang,[21] C.G.Yang,[8] H.J.Yang,[8] M.Yang,[8] J.B.Ye,[21] S.C.Yeh,[52] J.M.You,[35] An.Zalite,[38] Yu.Zalite,[38] P.Zemp,[49] Y.Zeng,[1] Z.P.Zhang,[21] B.Zhou,[12] G.Y.Zhu,[8] R.Y.Zhu,[33] A.Zichichi,[10,18,19] F.Ziegler,[48] G.Zilizi,[44,¶]

1 I. Physikalisches Institut, RWTH, D-52056 Aachen, FRG[§]
III. Physikalisches Institut, RWTH, D-52056 Aachen, FRG[§]
2 National Institute for High Energy Physics, NIKHEF, and University of Amsterdam, NL-1009 DB Amsterdam, The Netherlands
3 University of Michigan, Ann Arbor, MI 48109, USA
4 Laboratoire d'Annecy-le-Vieux de Physique des Particules, LAPP,IN2P3-CNRS, BP 110, F-74941 Annecy-le-Vieux CEDEX, France
5 Johns Hopkins University, Baltimore, MD 21218, USA
6 Institute of Physics, University of Basel, CH-4056 Basel, Switzerland
7 Louisiana State University, Baton Rouge, LA 70803, USA
8 Institute of High Energy Physics, IHEP, 100039 Beijing, China[△]
9 Humboldt University, D-10099 Berlin, FRG[§]
10 University of Bologna and INFN-Sezione di Bologna, I-40126 Bologna, Italy
11 Tata Institute of Fundamental Research, Bombay 400 005, India
12 Boston University, Boston, MA 02215, USA
13 Northeastern University, Boston, MA 02115, USA
14 Institute of Atomic Physics and University of Bucharest, R-76900 Bucharest, Romania
15 Central Research Institute for Physics of the Hungarian Academy of Sciences, H-1525 Budapest 114, Hungary[‡]
16 Massachusetts Institute of Technology, Cambridge, MA 02139, USA
17 INFN Sezione di Firenze and University of Florence, I-50125 Florence, Italy
18 European Laboratory for Particle Physics, CERN, CH-1211 Geneva 23, Switzerland
19 World Laboratory, FBLJA Project, CH-1211 Geneva 23, Switzerland
20 University of Geneva, CH-1211 Geneva 4, Switzerland
21 Chinese University of Science and Technology, USTC, Hefei, Anhui 230 029, China[△]
22 SEFT, Research Institute for High Energy Physics, P.O. Box 9, SF-00014 Helsinki, Finland
23 University of Lausanne, CH-1015 Lausanne, Switzerland
24 INFN-Sezione di Lecce and Universitá Degli Studi di Lecce, I-73100 Lecce, Italy
25 Los Alamos National Laboratory, Los Alamos, NM 87544, USA
26 Institut de Physique Nucléaire de Lyon, IN2P3-CNRS,Université Claude Bernard, F-69622 Villeurbanne, France
27 Centro de Investigaciones Energeticas, Medioambientales y Tecnologicas, CIEMAT, E-28040 Madrid, Spain[♭]
28 INFN-Sezione di Milano, I-20133 Milan, Italy
29 Institute of Theoretical and Experimental Physics, ITEP, Moscow, Russia
30 INFN-Sezione di Napoli and University of Naples, I-80125 Naples, Italy
31 Department of Natural Sciences, University of Cyprus, Nicosia, Cyprus
32 University of Nijmegen and NIKHEF, NL-6525 ED Nijmegen, The Netherlands
33 California Institute of Technology, Pasadena, CA 91125, USA
34 INFN-Sezione di Perugia and Universitá Degli Studi di Perugia, I-06100 Perugia, Italy
35 Carnegie Mellon University, Pittsburgh, PA 15213, USA
36 Princeton University, Princeton, NJ 08544, USA
37 INFN-Sezione di Roma and University of Rome, "La Sapienza", I-00185 Rome, Italy
38 Nuclear Physics Institute, St. Petersburg, Russia
39 University and INFN, Salerno, I-84100 Salerno, Italy
40 University of California, San Diego, CA 92093, USA
41 Dept. de Fisica de Particulas Elementales, Univ. de Santiago, E-15706 Santiago de Compostela, Spain
42 Bulgarian Academy of Sciences, Central Lab. of Mechatronics and Instrumentation, BU-1113 Sofia, Bulgaria
43 Center for High Energy Physics, Adv. Inst. of Sciences and Technology, 305-701 Taejon, Republic of Korea
44 University of Alabama, Tuscaloosa, AL 35486, USA
45 Utrecht University and NIKHEF, NL-3584 CB Utrecht, The Netherlands
46 Purdue University, West Lafayette, IN 47907, USA
47 Paul Scherrer Institut, PSI, CH-5232 Villigen, Switzerland
48 DESY-Institut für Hochenergiephysik, D-15738 Zeuthen, FRG
49 Eidgenössische Technische Hochschule, ETH Zürich, CH-8093 Zürich, Switzerland
50 University of Hamburg, D-22761 Hamburg, FRG
51 National Central University, Chung-Li, Taiwan, China
52 Department of Physics, National Tsing Hua University, Taiwan, China
§ Supported by the German Bundesministerium für Bildung, Wissenschaft, Forschung und Technologie
‡ Supported by the Hungarian OTKA fund under contract numbers T019181, F023259 and T024011.
¶ Also supported by the Hungarian OTKA fund under contract numbers T22238 and T026178.
♭ Supported also by the Comisión Interministerial de Ciencia y Tecnología.
♯ Also supported by CONICET and Universidad Nacional de La Plata, CC 67, 1900 La Plata, Argentina.
♮ Supported by Deutscher Akademischer Austauschdienst.
♢ Also supported by Panjab University, Chandigarh-160014, India.
△ Supported by the National Natural Science Foundation of China.

ISR $\geq$ 30 GeV	10.2%
$e^+e^- \to W^+W^- \to f\,f'f\,f'$	11.7%
$e^+e^- \to$ 2-photon	2.6%
$e^+e^- \to \tau^+\tau^-$	0.2%
$e^+e^- \to ZZ \to f\,f'f\,f'$	0.6%
$e^+e^- \to Ze^+e^- \to f\,f'e^+e^-$	0.6%

Table 1: Expected background fraction of the selected event sample.

$< 1-T >$	$0.0547 \pm 0.0016 \pm 0.0015$
$< \rho >$	$0.0440 \pm 0.0014 \pm 0.0009$
$< B_{\mathrm{T}} >$	$0.0936 \pm 0.0017 \pm 0.0018$
$< B_{\mathrm{W}} >$	$0.0670 \pm 0.0014 \pm 0.0013$
$< C >$	$0.2189 \pm 0.0051 \pm 0.0074$

Table 2: Mean values of thrust, T, scaled heavy jet mass, ρ, total jet broadening, B_{T}, wide jet broadening, B_{W}, and C parameter measured at $\sqrt{s} = 183$ GeV. The first error is statistical and the second is systematic.

	$(1-T)$	ρ	B_{T}	B_{W}	C
$\alpha_{\mathrm{s}}(183$ GeV)	0.1135	0.1070	0.1112	0.1028	0.1072
Fit Range	0.00−0.30	0.00−0.20	0.00−0.25	0.00−0.20	0.05−0.50
χ^2/d.o.f.	4.8 / 11	4.2 / 13	18.3 / 13	4.9 / 13	6.1 / 8
Statistical error	±0.0024	±0.0023	±0.0018	±0.0016	±0.0032
Systematic error	±0.0018	±0.0023	±0.0012	±0.0011	±0.0015
Overall experimental error	±0.0030	±0.0033	±0.0022	±0.0019	±0.0035
Overall theoretical error	±0.0055	±0.0038	±0.0065	±0.0058	±0.0052
Fit Range (for checking)	0.025−0.300	0.015−0.225	0.040−0.240	0.030−0.210	0.10−0.50

Table 3: α_{s} (183 GeV) from the fits to the event shape variables together with the estimated experimental and theoretical errors, fit ranges and fit qualities. The fit range for checking the fit qualities is also given in the last row.

Uncertainty due to	$(1-T)$	ρ	B_{T}	B_{W}	C
Fragmentation Model	±0.0028	±0.0016	±0.0024	±0.0014	±0.0034
Model parameters	±0.0019	±0.0016	±0.0013	±0.0038	±0.0013
Hadronisation	±0.0028	±0.0016	±0.0024	±0.0038	±0.0034
QCD scale	±0.0047	±0.0034	±0.0060	±0.0040	±0.0040
Matching scheme	±0.0026	±0.0028	±0.0043	±0.0044	–
Higher orders	±0.0047	±0.0034	±0.0060	±0.0044	±0.0040
Overall	±0.0055	±0.0038	±0.0065	±0.0058	±0.0052

Table 4: Contributions to the estimated theoretical errors for α_{s} determination. α_{s} has been determined from the C-parameter using log-R and R matching schemes and are found to differ by 0.0012. The other matching schemes have not been tried out and so the matching scheme uncertainty cannot be determined for α_{s} as determined from C-parameter.

Variable		Value	Error	
			Statistical	Systematic
First moment	$(\mu_1 = < N_{\mathrm{ch}} >)$	27.04	0.24	0.43
Second Moment	$(\mu_2 = < N_{\mathrm{ch}}^2 >)$	802	15	25
Third Moment	$(\mu_3 = < N_{\mathrm{ch}}^3 >)$	25.9×10^3	0.7×10^3	1.3×10^3
Dispersion	$(\mathrm{D} = \sqrt{\mu_2 - \mu_1^2})$	8.43	0.18	0.18
Skewness	$(\mathrm{S} = [\mu_3 - 3\mu_1\mu_2 + 2\mu_1^3]/\mathrm{D})$	0.58	0.18	0.09

Table 5: Moments of charged multiplicity distribution together with dispersion and skewness

$\sqrt{s}$	$\xi^\star$ Value	Error on $\xi^\star$	
		Statistical	Systematic
133 GeV	3.90	0.04	0.05
163 GeV	3.92	0.05	0.04
172 GeV	4.06	0.05	0.05
183 GeV	4.08	0.02	0.04

Table 6: $\xi^\star$ values determined at different centre-of-mass energies

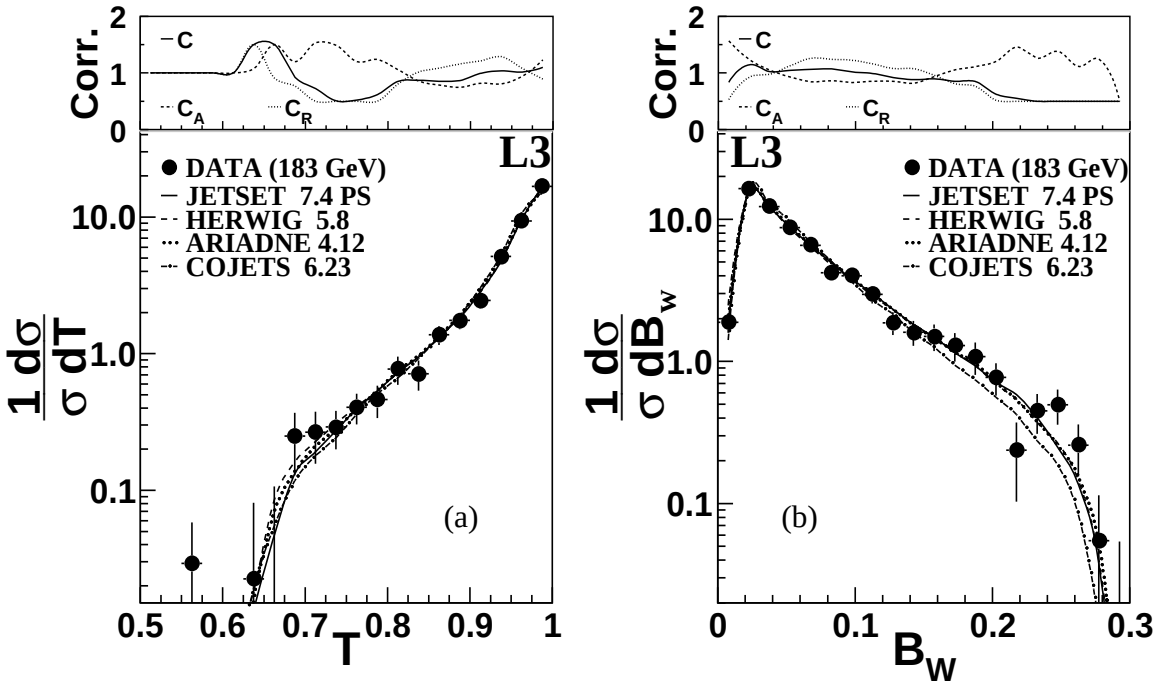

Figure 1: Corrected distributions at $\sqrt{s} = 183$ GeV of (a) thrust, T, and (b) wide jet broadening, B_{W}, in comparison with QCD model predictions. The errors shown are statistical only. The correction factors due to resolution, C_R, acceptance, C_A, and overall are also shown.

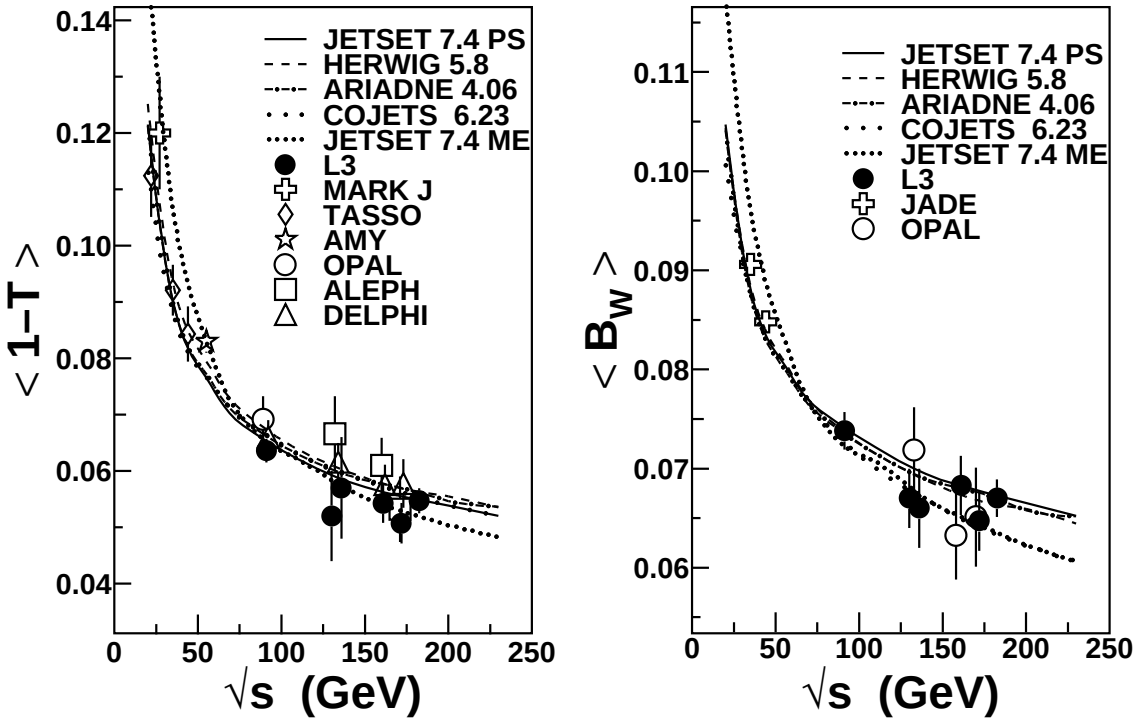

Figure 2: Distribution of mean 1−thrust, $< 1 - T >$ and wide jet broadening, $< B_{\mathrm{W}} >$ as a function of the centre-of-mass energy, compared to several QCD models.

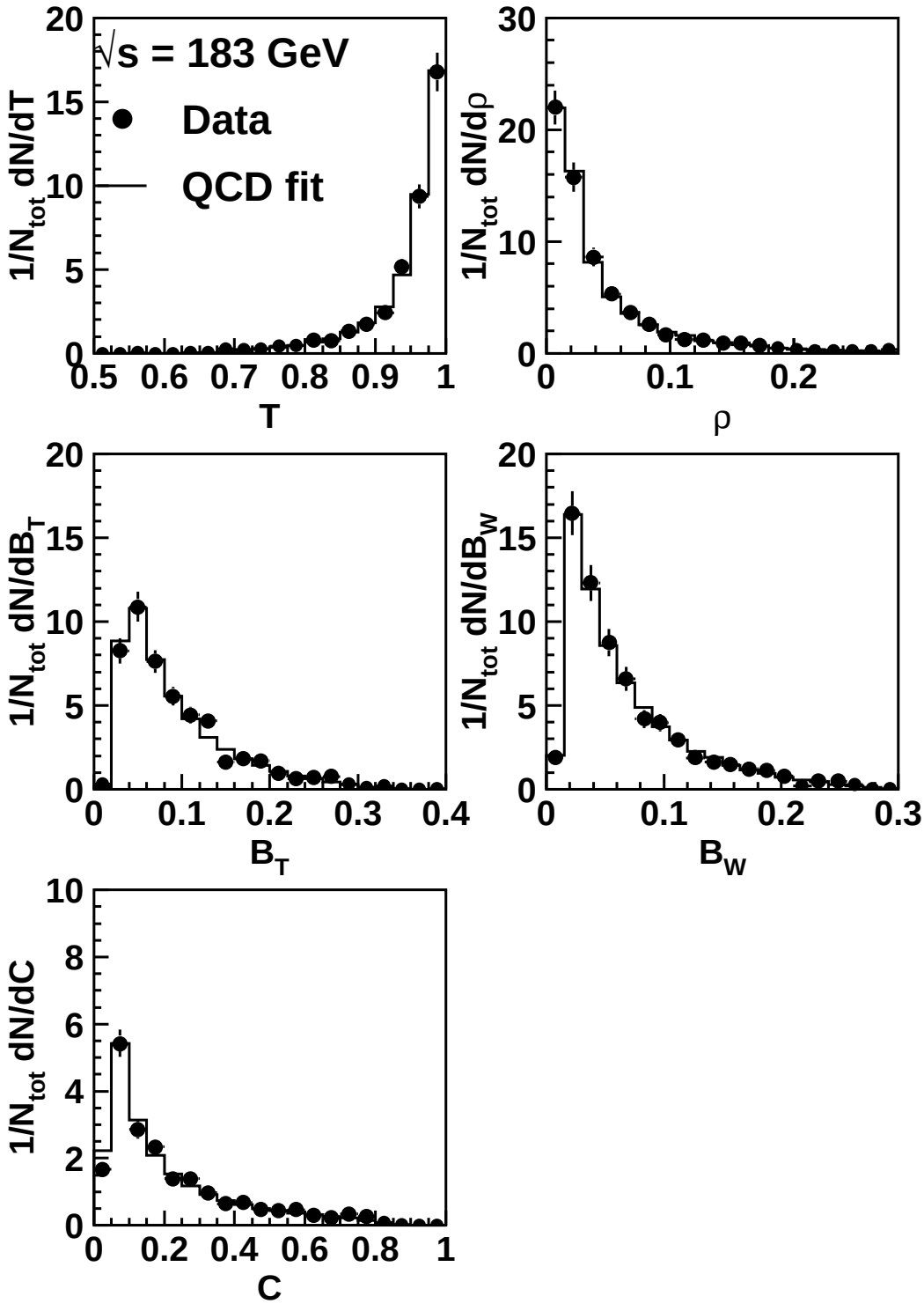

Figure 3: Measured distributions of thrust, T, scaled heavy jet mass, ρ, total, B_{T}, and wide, B_{W}, jet broadening, and C parameter in comparison with QCD predictions at 183 GeV. The experimental errors include statistical and systematic uncertainties.

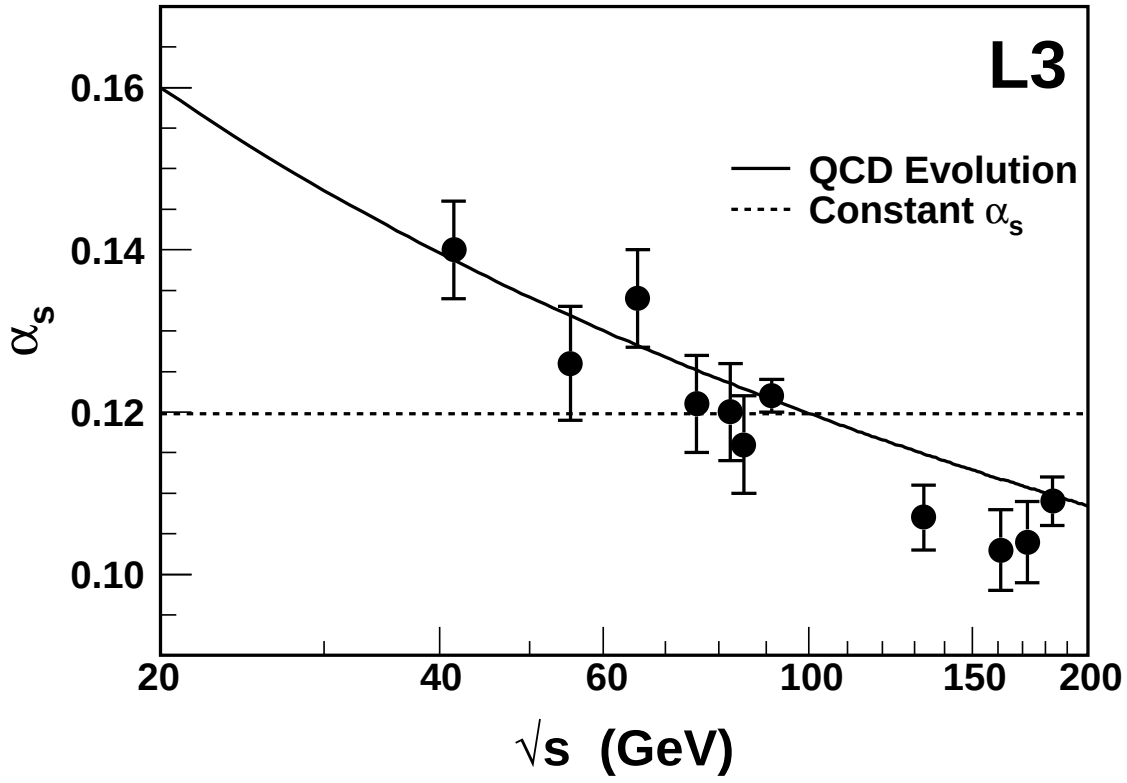

Figure 4: α_s measurements from event shape distributions as a function of the centre-of-mass energy. The errors shown are only experimental. The points below 91 GeV have been obtained from radiative hadronic events. The solid and dashed lines are fits of the data points with the energy dependence of α_s as given by QCD and with constant α_s, respectively.

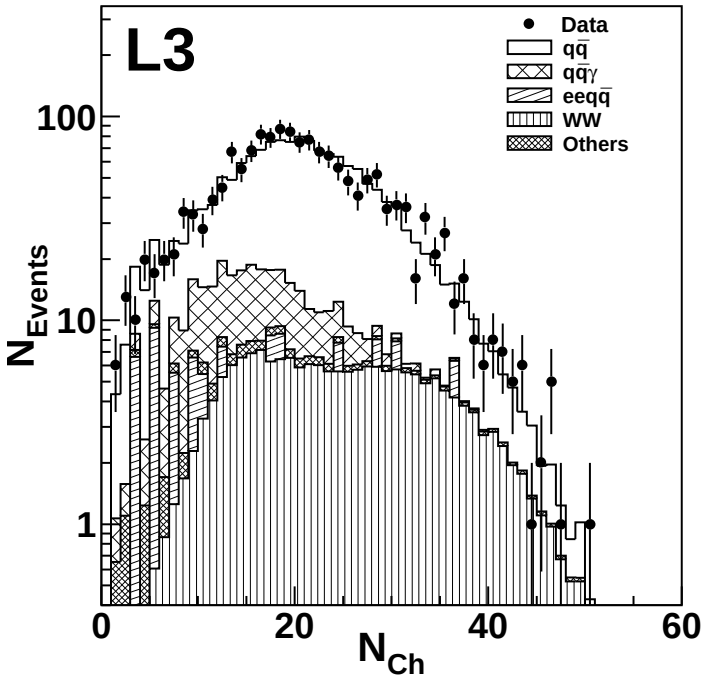

Figure 5: Measured charged particle multiplicity distribution at $\sqrt{s} = 183$ GeV compared with expectation from signal and background processes.

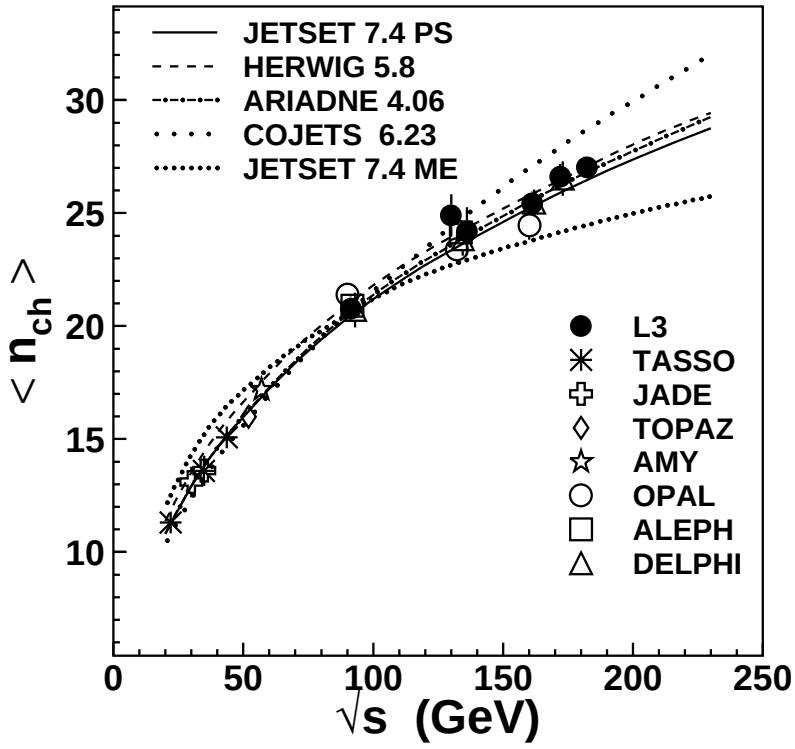

Figure 6: The mean charged particle multiplicity, $\langle n_{ch} \rangle$, as a function of the centre-of-mass energy, compared to several QCD Models.

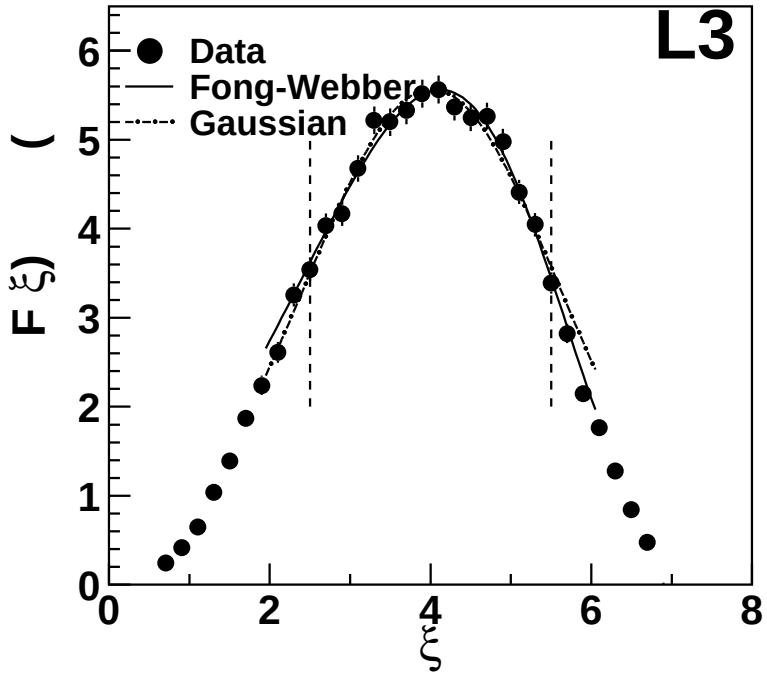

Figure 7: Corrected ξ-spectrum at $\sqrt{s} = 183$ GeV together with the fits to Gaussian and skewed Gaussian distributions. The fit range is between the vertical lines.

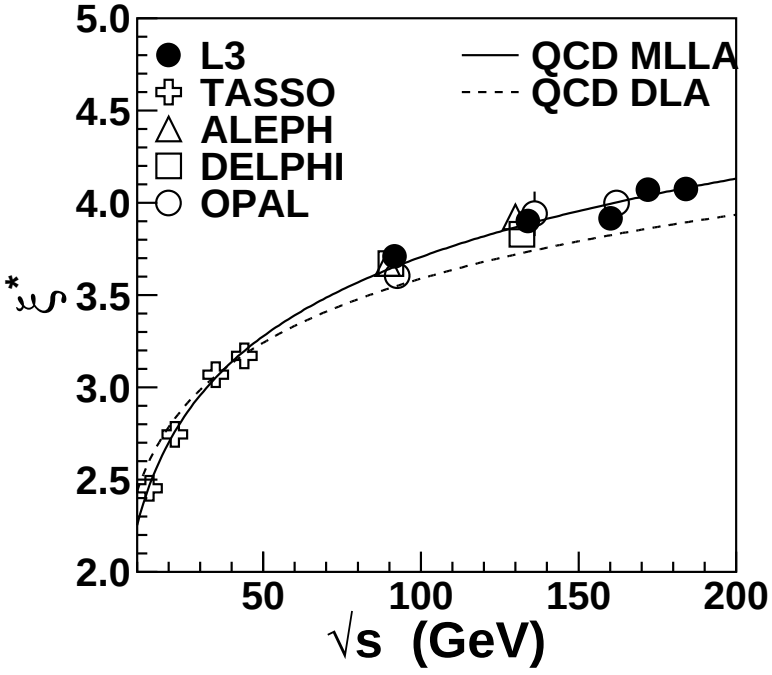

Figure 8: Energy evolution of ξ^*: the solid and dashed lines are fits to the L3 and TASSO data with Modified Leading Log Approximation (MLLA) and Double Leading log Approximation (DLA) of QCD.